

- MHD-Flows and Turbulence, Bat-Sheva, Israel (1978).
14. M. Petrick, P. F. Dunn, E. S. Pierson, P. V. Dauzvardis and I. Pollack, liquid-metal MHD energy conversion, March 1976 to September 1977 Status Report, Argonne National Laboratory Report, ANL/MHD 78-5 (1978).
  15. M. Petrick and K. Y. Lee, Performance characteristics of liquid-metal MHD generator, in *Proc. Symp. on MHD Elec. Power Gen.*, Vol. 2, pp. 953-970 (1964).
  16. P. S. Lykoudis, Shunt-layer thickness, Argonne National Laboratory LMMHD Group Memo 77-2 (1977).
  17. G. B. Wallis, *One-Dimensional Two-Phase Flow*, McGraw-Hill, New York (1969).
  18. H. Branover, *Magnetohydrodynamic Flow in Ducts*, Wiley, New York (1969).
  19. M. Petrick, Two-phase flow liquid-metal MHD generator, in *MHD Flows and Turbulence*, pp. 125-245, Wiley, New York (1976).

*Int. J. Heat Mass Transfer.* Vol. 23, pp. 1690-1693  
Pergamon Press Ltd. 1980. Printed in Great Britain

## A NOTE ON MASS TRANSFER IN TURBULENT WALL JETS

V. KUPPU RAO

Department of Mechanical Engineering, Indian Institute of Science,  
Bangalore 560012, India

(Received 20 August 1979 and in revised form 1 April 1980)

### NOMENCLATURE

$a$ ,	exponent;	$\delta$ ,	boundary layer thickness (for wall jets $\delta$ is the height at which $u = U_M/2$ );
$A$ ,	constant;	$\delta_c$ ,	concentration boundary layer thickness;
$b$ ,	exponent;	$\delta_M$ ,	height at which $u = U_M$ ;
$B$ ,	constant;	$\eta$ ,	similarity parameter ( $y/\delta$ );
$c$ ,	mass concentration;	$\eta_M$ ,	value of $\eta$ at which $u = U_M$ ;
$c_0$ ,	mass concentration at the surface of the porous plate;	$\zeta$ ,	similarity parameter ( $y/\delta_c$ );
$d_0$ ,	width of nozzle (PWJ); diameter of nozzle (RWJ);	$u', v', c'$ ,	turbulent fluctuations in $u, v$ and $c$ ;
$E$ ,	constant;	$\rho$ ,	density;
$F$ ,	non-dimensional stream function;	$\nu$ ,	kinematic viscosity;
$G$ ,	non-dimensional concentration;	$\tau_0$ ,	wall shear stress;
$K$ ,	exchange coefficient;	$\tau$ ,	shear stress;
$u$ ,	mean velocity in the direction of flow;	$e_M$ ,	diffusivity of momentum (turbulent);
$U_M$ ,	maximum velocity (wall Jet);	$e_m$ ,	diffusivity of mass (turbulent);
$U_0$ ,	nozzle exit velocity;	$Re_0$ ,	Reynolds number at nozzle exit = $U_0 d_0 / \nu$ ;
$v$ ,	mean velocity in the transverse direction;	$Sc_t$ ,	turbulent Schmidt number.
$x$ ,	longitudinal coordinate;		
$x_0$ ,	distance of leading edge of porous plate from the virtual origin;		
$y$ ,	transverse coordinate;		
$y_0$ ,	height of nozzle above flat plate—radial wall jet;		

### 1. INTRODUCTION

THE PROCESS of mass transfer from saturated porous surfaces exposed to turbulent air streams finds many practical applications. In many cases, the air stream will be in the form of a wall jet over the porous surface. The aerodynamics of both

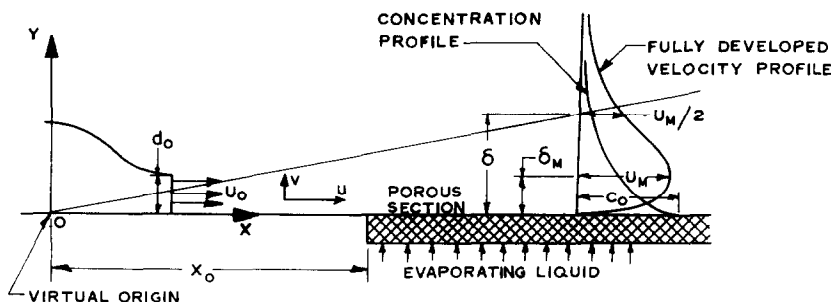


FIG. 1(a). Two-dimensional plane wall jet.

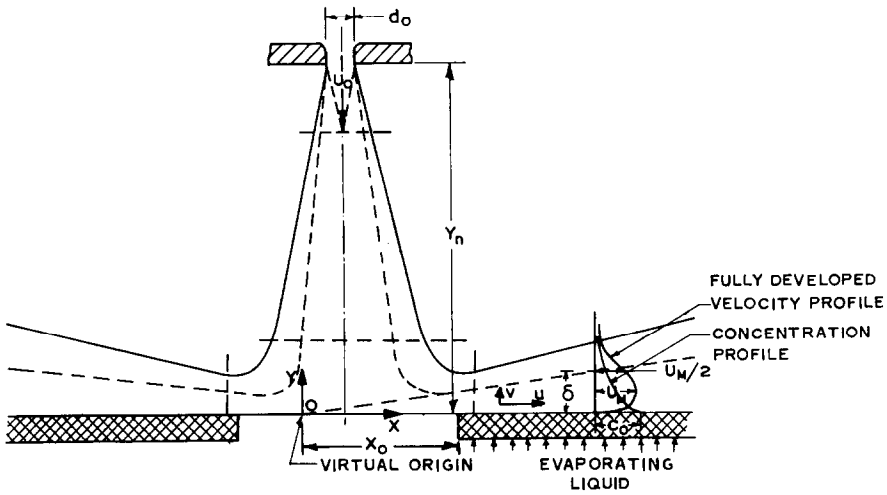


FIG. 1(b). Radial wall jet.

FIG. 1. Schematic representation of the plane and the radial wall jets with mass transfer.

plane and radial wall jets have been investigated in detail and a vast amount of literature is available on the subject [1-3]. On the other hand, mass transfer studies in turbulent wall jets are meagre. Mass transfer in both plane and radial wall jets, as shown schematically in Fig. 1, is considered herewith. 'Similarity solutions' to the governing equations are obtained and

experimental evidence is presented which indicates that the concentration profiles are also self-preserving.

2. THEORETICAL ANALYSIS

The governing equations for the flow under consideration (with reference to Fig. 1) are:

$$\text{Continuity} \quad \frac{\partial}{\partial x}(ux^j) + \frac{\partial}{\partial y}(vx^j) = 0 \quad (1)$$

$$\text{Momentum} \quad u \frac{\partial u}{\partial x} + v \frac{\partial u}{\partial y} = \frac{\partial}{\partial y} \left( \frac{\tau}{\rho} \right) \quad (2)$$

$$\text{Conservation} \quad u \frac{\partial c}{\partial x} + v \frac{\partial c}{\partial y} = - \frac{\partial}{\partial y} (\dot{m}''') \quad (3)$$

where

$$j = 1, \text{ for the radial wall jet}$$

$$j = 0, \text{ for the plane wall jet}$$

and

$$\frac{\tau}{\rho} = \left[ v \frac{\partial u}{\partial y} - \overline{u'v'} \right]$$

$$\dot{m}''' = \left[ -D \frac{\partial c}{\partial y} + \overline{v'c'} \right].$$

Considering the momentum equation first, we seek a similarity solution for it by introducing the following:

1. Power law variation for the wall jet thickness  $\delta$  and the maximum velocity  $U_m$  at any section given by  $U_M = Ax^a, \delta = Bx^b, x$  being measured from a 'virtual origin'.
2. A similarity parameter  $\eta = y/\delta = y/Bx^b$
3. The self-preserving velocity profile  $u/U_M = f(\eta)$
4. Representation of the shear stress as

$$\frac{\tau}{\rho} \approx -\overline{u'v'} = -U_M^2 h_1(\eta).$$

The continuity equation is eliminated by introducing the stream function  $\psi$  such that

$$u = \frac{1}{x^j} \frac{\partial \psi}{\partial y}; \quad v = -\frac{1}{x^j} \frac{\partial \psi}{\partial x}.$$

The stream function at any section  $x$  is then:

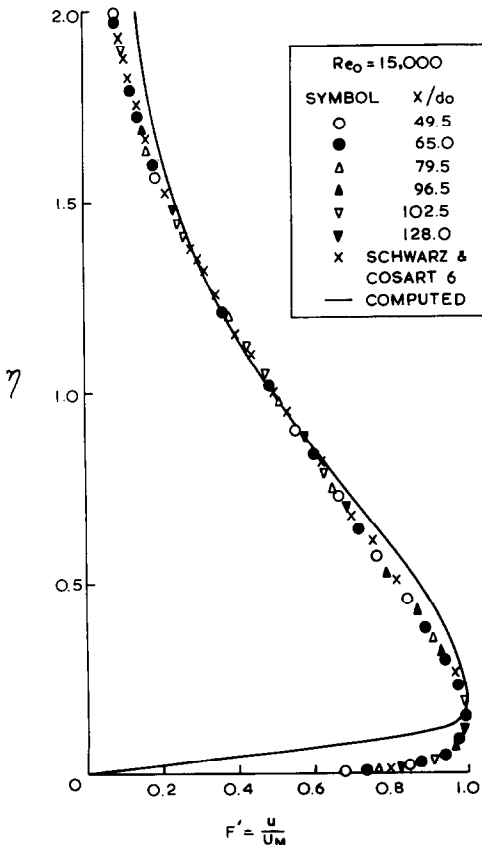


FIG. 2. Non-dimensional velocity profile. Two-dimensional plane wall jet.

$$\psi = \int_0^y u x^j dy = ABx^{a+b+j} \int_0^\eta f(\eta) d\eta = ABx^{a+b+j} F(\eta).$$

With these substitutions the momentum equation (2) turns out as

$$A^2 a x^{2a-1} F'^2 - A^2 (a+b+j) x^{2a-1} FF'' = -\frac{A^2}{B} x^{2a-b} h_1'. \tag{4}$$

where, the primes designate differentiation with respect to  $\eta$ . The dimensional homogeneity of equation (4) implies that  $b = 1$  both for the plane wall jet and the radial wall jet.

Consider now the momentum integral equation for these flows. This can be written as

$$\frac{d}{dx} \int_0^y u^2 x^j dy + \frac{\tau_0}{\rho} x^j = 0$$

or on integration with respect to  $x$ ,

$$\int_0^y u^2 x^j dy + \int_0^x \frac{\tau_0}{\rho} x^j dx = \text{constant.} \tag{5}$$

It is now necessary to assume that the viscous dissipation term in the momentum integral equation is small compared to the total momentum of the jet. This assumption may be justified on the ground that the minimum value of the ratio of total momentum in the jet to the viscous dissipation at the wall as calculated from the experimentally measured profiles is of the order of 25 : 1 for the plane wall jet and 40 : 1 for the radial wall jet indicating a slow rate of momentum decay in wall jets [5]. Then equation (5) becomes

$$\int_0^y u^2 x^j dy = \text{constant}$$

or

$$A^2 B x^{2a+b+j} \int_0^\infty F'^2 d\eta = \text{constant.} \tag{6}$$

The dimensional homogeneity of equation (6) implies  $a = -\frac{1}{2}$  for the plane wall jet and  $a = -1$  for the radial wall jet. It may be mentioned that the values of  $a$  and  $b$  thus obtained are in good agreement with those obtained from experimental data of other investigators [4].

With these values of  $a$  and  $b$ , the momentum equation reduces to

$$F'^2 + FF'' = \frac{(2-j)}{B} h_1'. \tag{7}$$

Next, consider the mass conservation equation. Here we may anticipate similarity of concentration profiles with respect to another parameter  $\zeta$  defined by

$$\zeta = \frac{y}{E(x-x_0)}$$

where,  $E$  is a constant. Following the method used to transform the momentum equation we write the self preserving concentration profile as

$$c/c_0 = G(\zeta)$$

and

$$\dot{m}'' \approx v'c' = U_M c_0 h_2(\zeta)$$

where,  $c_0$  is the concentration of vapour along the surface of the plate (taken to be constant). The introduction of these into the mass conservation equation results in

$$\frac{FG^*}{(2-j)} = \frac{h_2^*}{B} \tag{8}$$

where \* designates differentiation with respect to  $\zeta$ . It can be

easily shown that for a fixed value of  $x_0$ , the above equation can also be written as

$$\frac{FG'}{(2-j)} = \frac{h_2'}{B} \tag{9}$$

the primes, as before, denoting differentiation with respect to  $\eta$ .

Before, this set of non-linear ordinary differential equations (7) and (9) can be solved, a particular turbulent diffusion hypothesis has to be selected to connect  $h_1$  and  $h_2$  with  $F$ ,  $G$  and their derivatives. There are many empirical hypothesis of turbulent transport none of which, however, is entirely satisfactory. For purposes of illustration, we choose the 'constant exchange coefficient' hypothesis (Prandtl) and write

$$\frac{\tau}{\rho} = \epsilon_M \frac{\partial u}{\partial y} = K \delta U_M \frac{\partial u}{\partial y} \tag{10}$$

and

$$-\dot{m}'' = \epsilon_m \frac{\partial c}{\partial y} = \frac{\epsilon_M}{Sc_t} \frac{\partial c}{\partial y} = \frac{K \delta U_M}{Sc_t} \frac{\partial c}{\partial y}. \tag{11}$$

Substituting relations (10) and (11), equations (7) and (9) turn out as

$$(2-j) \frac{K}{B} F''' + FF'' + F'^2 = 0 \tag{12}$$

$$(2-j) \frac{K}{BS_c t} G'' + FG' = 0. \tag{13}$$

It is not possible to have a closed form solution of this set of non-linear ordinary differential equations with conditions

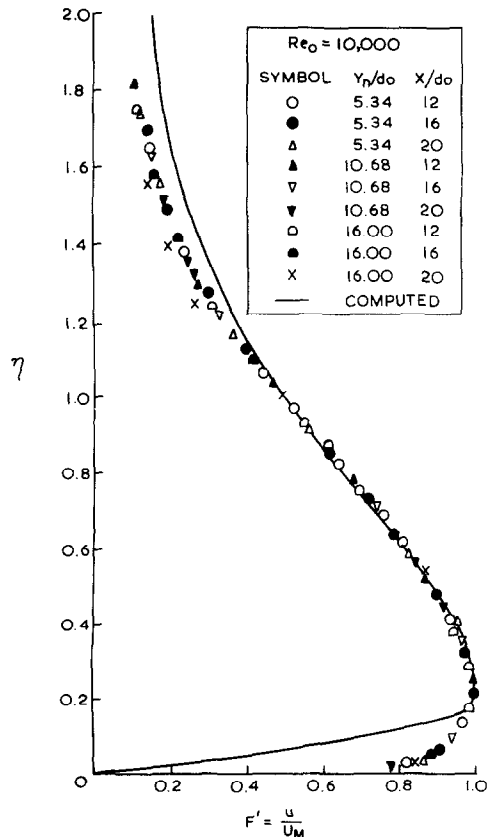


FIG. 3. Non-dimensional velocity profile. Radial wall jet.

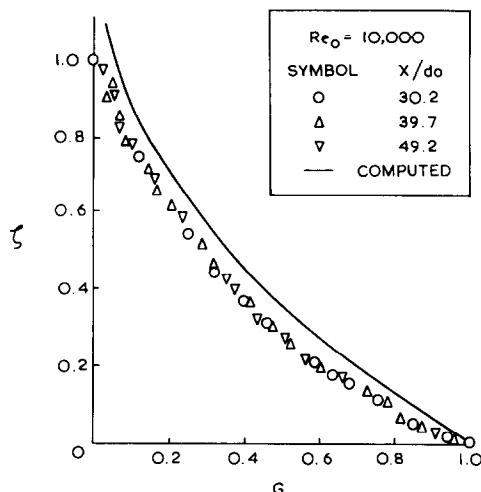


FIG. 4. Non-dimensional concentration profile. Plane wall jet.

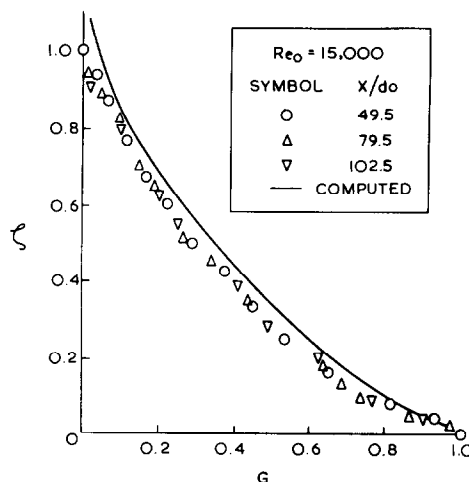


FIG. 5. Non-dimensional concentration distribution. Radial wall jet.

specified at two boundaries. Therefore, a numerical solution was obtained using the Runge-Kutta method.

Equations (12) and (13) can be written as

$$F''' = \frac{1}{\lambda}(FF'' + F'^2) \quad (14)$$

$$G'' = \frac{Sc_t}{\lambda} FG' = \frac{1}{\lambda} FG' \quad (\text{assuming } Sc_t = 1) \quad (15)$$

where  $\lambda = \text{constant}$ .

The momentum equation is independent of the mass conservation equation and can be solved by itself. In solving the momentum equation, the numerical integration was started by assuming  $F = F' = 0$  at  $\eta = 0$  (wall). Equating  $F(0) = 0$ , implies  $v = 0$  at the wall. This is approximately true in the present case as the evaporation rates were very small. Typical values of  $m''(0)$  and  $c_0$  were  $10^{-4} \text{ g cm}^{-2} \text{ s}$  and  $20 \times 10^{-4} \text{ g cm}^{-3}$  giving value of  $v = 0.05 \text{ cm s}^{-1}$  at the wall. The values of  $\lambda$  and  $F''(0)$  were arrived at by trial and error to obtain the best fit of the computed curve of  $F'$  vs  $\eta$  with the experimental curve. The value of  $\lambda$  had to be changed in the outer layer again. For the plane wall jet, the values of  $\lambda$  selected were  $-0.011$  in the inner layer and  $-0.41$  in the outer layer. The corresponding values for the radial wall jet were  $-0.0158$  and  $-0.36$  respectively. These values of  $\lambda$  were then used in the integration of the mass conservation equation.

### 3. EXPERIMENTAL WORK

Two test rigs were fabricated; one for the plane wall jet and the other for the radial wall jet to simulate what is indicated in Figs. 1(a) and (b).

Smooth, homogeneously porous grade B 'Porosint' plates were used to evaporate methanol in the fully developed regions of the two turbulent wall jets. The concentrations of methanol at different distances and at different heights above the porous plates were measured by a gas chromatograph.

Mean velocity measurements in the wall jets were recorded by a narrow pilot tube coupled to a projection manometer. The fully developed mean velocity profiles in both cases exhibited 'similarity' and conformed quite closely to those given in literature.

Details of the experimental work can be found in [5].

### 4. RESULTS

The 'similar' velocity profiles of the plane wall jet and the radial wall jet are shown in Figs. 2 and 3. The computed profiles obtained by numerical integration of equation (12) are also indicated. The agreement between the computed profiles and the measured profiles is poor in the inner layer (between  $y = 0$  and  $y = \delta_M$ ) and improves in the outer region ( $y > \delta_M$ ). This is mainly due to the poor representation of eddy viscosity near the wall by the constant exchange coefficient hypothesis.

Figures 4 and 5 show the measured and the computed non-dimensional concentration profiles in the plane wall jet and the radial wall jet respectively. The agreement between the two is reasonably good considering the crude hypothesis of turbulent transport assumed. It can be seen that the concentration profiles at different sections do exhibit 'similarity' in both cases with respect to the similarity parameter  $\zeta$  as defined.

*Acknowledgement*—The author is grateful to Dr. M. Inderjit for help in the computation work and for providing the experimental data presented herewith.

### REFERENCES

1. J. W. Gauntner, J. N. B. Livingood and P. Hrycak, Survey of literature on flow characteristics of a single turbulent jet impinging on a flat plate, NASA TND-5652 (Feb. 1970).
2. N. Rajaratnam and K. Subramanya, An annotated bibliography of wall jets, Tech. Rep., Dept. of Civil Engineering, Univ. of Alberta, Edmonton (1967).
3. N. Rajaratnam, *Turbulent Jets*. Elsevier, Amsterdam (1976).
4. V. Kuppu Rao and M. Inderjit, Turbulent wall jets, *J. Ind. Inst. Sci.* **60**(1), 35-45 (1978).
5. M. Inderjit, Mass transfer studies in some types of turbulent flow, Ph.D., Thesis, Indian Institute of Science, Bangalore (1976).
6. W. H. Schwarz and W. P. Cosart, The two-dimensional turbulent wall jet, *J. Fluid Mech.* **10**, 481 (1961).